Nanoscale

Accepted Manuscript

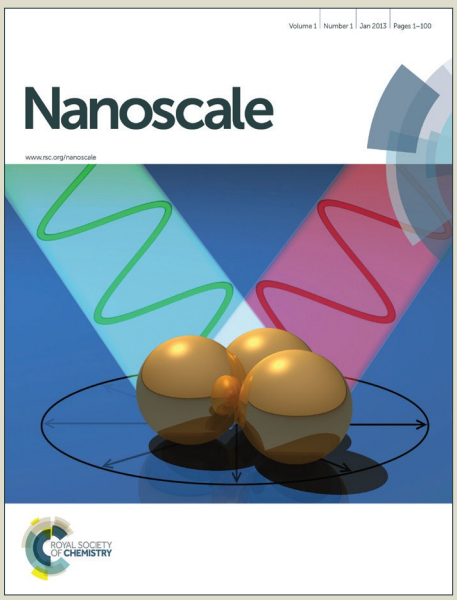

ROYAL SOCIETY OF CHEMISTRY

www.rsc.org/nanoscale

Transition of Radiative Recombination Channel from Delocalized States to Localized States in GaInP Alloy with Partial Atomic Ordering: A Direct Optical Signature of Mott Transition?

Z. C. Su,[a,b,c] J. Q. Ning,[a,b,c,d] Z. Deng,[a,b,c] X. H. Wang,[a,b,c] S. J. Xu,[*a,b,c] R. X. Wang,[d] S. L. Lu,[d] J. R. Dong[d] and H. Yang[d]

Anderson localization is a predominant phenomenon in condensed matter and materials physics. In fact, localized and delocalized states often co-exist in one material. They are separated by a boundary called the mobility edge. Mott transition may take place between these two regimes. However, it is widely recognized that an apparent demonstration of Anderson localization or Mott transition is a challenging task. In this article, we presents a direct optical observation of transition of radiative recombination dominant channel from delocalized (i.e., local extended) states to Anderson localized states in the GaInP base layer of a GaInP/GaAs single junction solar cell by the means of variable-temperature electroluminescence (EL) technique. It is found that by increasing temperature, we can boost a remarkable transition of radiative recombination dominant channel from the delocalized states to the localized states. The delocalized states are induced by the local atomic ordering domains (InP/GaP monolayer superlattices) while the localized states are caused by random distribution of indium (gallium) content. Efficient transfer and thermal redistribution of carriers between the two kinds of electronic states were revealed to result in distinct EL mechanism transition and electrical resistance evolution with temperature. Our study gives rise to a self-consistent precise picture for carrier localization and transfer in GaInP alloy that is an extremely technologically important energy material for fabricating high-efficiency photovoltaic devices.

[a]Department of Physics, [b]HKU-Shenzhen Institute of Research and Innovation (HKU-SIRI), and [c]HKU-CAS Joint Laboratory on New Materials, The University of Hong Kong, Pokfulam Road, Hong Kong, China. E-mail: sjxu@hku.hk

[d]Suzhou Institute of Nano-tech and Nano-bionics, Chinese Academy of Sciences, Suzhou 215123, China

Introduction

Nowadays, it is widely known that Anderson localization may take place in any practical crystalline solids with disorders and imperfections. Since Anderson's seminal theoretical paper in 1958,[1] actually, carrier localization has been a hot topic until present day.[2–15] However, it has been also known and widely recognized that it is not easy and even difficult to experimentally demonstrate Anderson localization in practical physical systems.[8–15] So far, apparent demonstration examples of Anderson localization could be the localization of electromagnetic waves (light) and matter waves of cold atoms.[8–12, 14, 15] On the other hand, localized states and delocalized (extended) states may simultaneously appear in one material. As a result, a so-called mobility edge may exist between them, and Mott transition may take place between the two regimes.[16] In terms of scientific significance of Anderson localization and Mott transition, seeking for experimental demonstration of Anderson localization in electronic systems is still an interesting enough issue. Partially disordered isovalent ternary semiconductors $A_xB_{1-x}C$ such as $In_xGa_{1-x}N$ and $Ga_xIn_{1-x}P$ may offer us a good chance to test Anderson's idea.[17–19] In particular, $Ga_xIn_{1-x}P$ (denoted as GaInP hereafter) alloy could be an excellent sample system for investigating Anderson localization of electronic states, because its ordering (disordering) degree can be controlled to some extent.[19–23] In partially ordered (disordered) GaInP alloy, local atomic ordering domians of InP/GaP monolayer superlattices are within disordered lattice matrix where Ga and In atoms are randomly distributed. Delocalized states may form within the local atomic ordering domains, whereas localized states may be caused by the random disorders of In and Ga atoms. If radiative recombination occurs from the delocalzied states and localized states simultaneously and respectively, we may obtain a treasure opportunity to optically "view" and examine the delocalized states and localized states in a solid material. Furthermore, optical signature of Mott transition between the two regimes may be observed in GaInP alloy.

On the other hand, GaInP alloy is a technologically important energy material for fabricating high-efficiency solar cells and efficient visible light emitting diodes (LEDs) for solid-state lighting.[24, 25] Therefore, understanding carrier behaviors and optical properties of GaInP is vital for improving the performance of GaInP-based solar cells and LEDs. It has been confirmed by Smith *et al*. using spatially resolved photoluminescence (PL) measurements that GaInP contains a statistical distribution of domains with different degrees of spontaneous ordering.[26] Our recent study on polarized PL spectra in GaInP alloy has revealed that the emission spectrum contains both completely polarized and non-polarized components, originating from the radiative recombination of carriers in ordered domains and disordered regions, respectively.[19] Moreover, the effect of carrier localization in the GaInP base layer on the performance of GaInP/GaAs double-junction solar cells has been discussed.[27] However, to the best of our knowledge, very few studies have been devoted to the experimental demonstration of carrier transition from delocalized states to localized states in a solid material. In this article, we report a clear optical demonstration of carrier transition from delocalized states to Anderson-type localized states in partially ordered GaInP alloy utilizing temperature-dependent electroluminescence (EL)

measurements. Such a firm demonstration originates from the observation of transition of main luminescence channel from the two kinds of electronic states in the GaInP base layer of a GaInP/GaAs single junction solar cell structure under a constant electrical injection. Significant thermally redistribution of carriers between the two kinds of electronic states results in the transition of luminescence mechanism. On the basis of localized-state ensemble (LSE) luminescence model, an effective thermal activation barrier was deduced to characterize the boundary separating the two groups of states. The electrical resistance of the cell was also found to show distinct temperature dependence predicted by theory of Anderson localization.

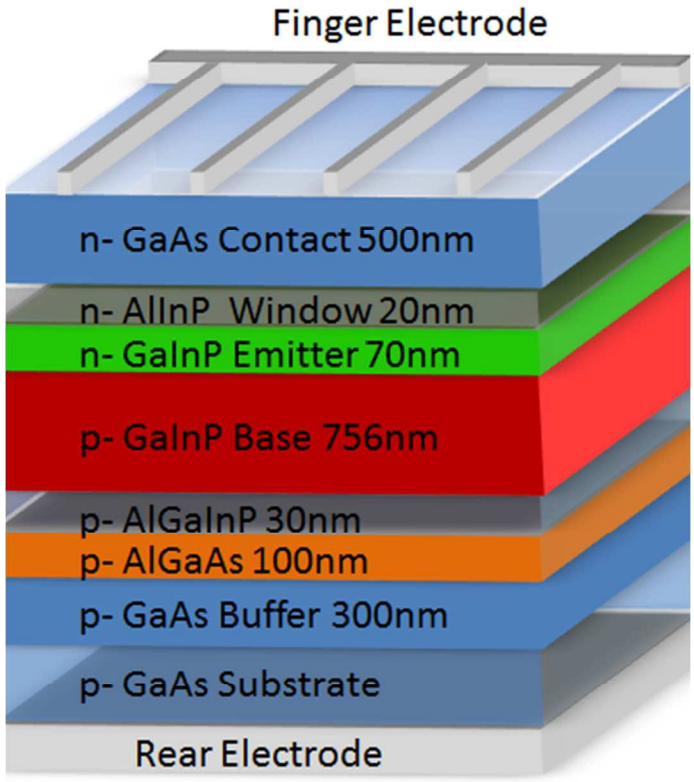

Fig. 1. Schematic diagram of the structural details of the studied GaInP/GaAs solar cell.

Experimental details

The GaInP/GaAs solar cell examined in this study was grown by the technique of low pressure metal-organic chemical vapor deposition. The detailed constitution of the grown solar cell is schematically shown in Fig. 1. The GaInP base layer is 756 nm thick while the emitter layer is 70 nm. In our previous work, we have already shown that the red color luminescence stems from the

GaInP base layer.[28] In the EL measurement, the solar cell sample was mounted on the cold finger of a Janis closed cycle cryostat with temperature controllable from 8 to 300 K, and biased with an Aim-TTi TSX3510P DC power supply. The EL luminescence was dispersed by an Acton SP 300i monochromator and finally detected with a Hamamatsu R928 photomultiplier tube. A Stanford Research lock-in amplifier (SR830) was used with a chopper to achieve high signal-to-noise ratio.

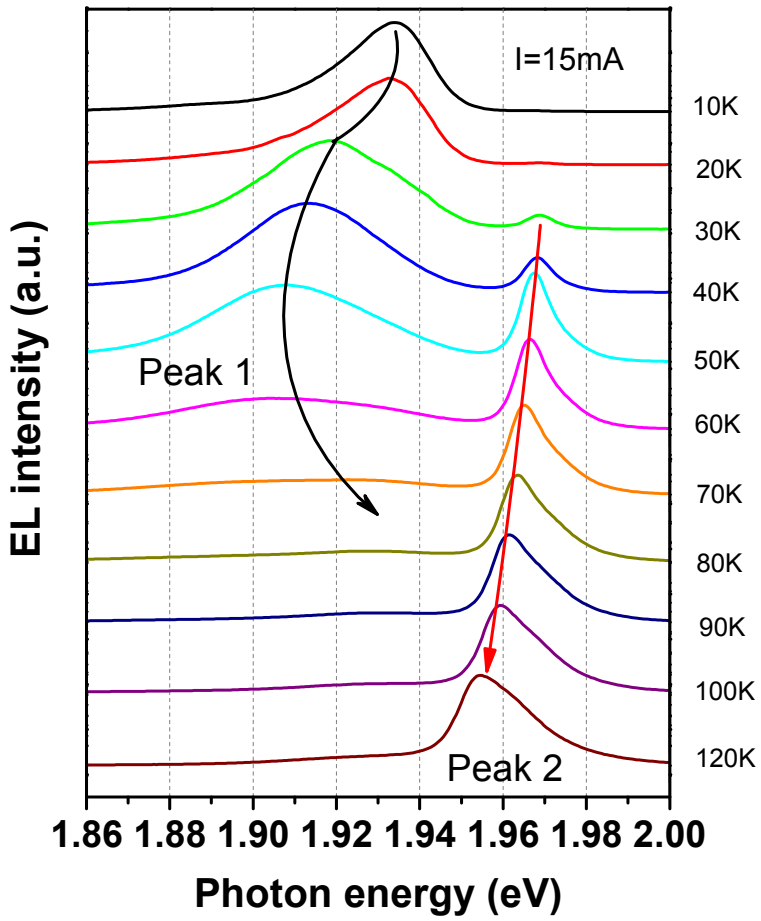

Fig. 2. Measured EL spectra of the sample at different temperatures and under the constant electrical injection current of 15 mA. For clarity, the spectra were shifted vertically.

Results and discussion

The EL experiments were performed on the GaInP/GaAs solar cell at different temperatures and under a constant injection current of 15 mA. Figure 2 shows the EL spectra measured from the

sample at different temperatures. As shown in this figure, only one broad peak (marked as Peak 1) centering at 641 nm is observed when the temperature is below 20 K. As the temperature goes higher than 20 K, another peak located at the high-energy side, denoted as Peak 2, gets observable. Peak 2 is centered at 630 nm at 30 K, and its peak position shows a gradual red shift with increasing the temperature. Peak 1 is dominant in the EL spectra in the temperature range from 10 K to 50 K, but its intensity decreases quickly and quenches at about 80 K. On the other hand, Peak 2 becomes dominant at higher temperatures. Besides the change in the intensity of the two emission peaks, their line shapes also show interesting changes as the temperature increases. For example, Peak 1 exhibits an asymmetric line shape with long low-energy tail at low temperatures, showing the typical feature of localized state luminescence. In contrast, Peak 2 displays an asymmetric line shape with long high-energy tail at high temperatures while it shows symmetric line shape at temperatures < 60 K. In order to further inspect the spectral behaviors of the two emission peaks, their peak positions (solid symbols) versus temperature are plotted in Fig. 3. As seen from the data in Fig. 3, the temperature evolution of the peak position of Peak 2 follows the red shift tendency (solid curve) described by the Varshni's empirical formula, whereas that of peak 1 shows a V-shaped evolution, red shifted first and then blue shifted. These large differences in spectral features suggest that the two emission peaks may originate from very different electronic states: two kinds of electronic states with dissimilar properties. It is known that spontaneous partial ordering in GaInP alloy can result in local atomic ordering domains embedded inside the remaining disordered region. These local ordering domains consisting of alternative InP/GaP monolayer superlattice-like structures may have varying degrees of ordering,[26] leading to local extended states (delocalized states) with a broad energy distribution. It should be noted that such local extended states still have lower potential energy minima compared with the band gap of the disordered region. On the other hand, another kind of electronic states may form in the remaining disordered region where Ga and In atoms randomly fluctuate. In terms of Anderson localization concept,[1] the second kind of electronic states formed in the disordered region shall be localized states. Thanks to the direct band gap nature of GaInP alloy, radiative recombination of carriers occupying the two kinds of electronic states may produce the two separate emission bands with very dissimilar properties including different peak energy (central wavelength), lineshape, and even polarization.[18] Indeed, as mentioned in the introduction section, we have measured the polarization of the photoluminescence signal from an unbiased GaInP epilayer with partial atomic ordering grown on GaAs, and unambiguously demonstrate that the emission spectrum contains both completely polarized and non-polarized components, originating from the radiative recombination of electron-hole pairs quantum-mechanically confined in the superlatice-like ordered domains and remaining disordered regions, respectively.[19] Moreover, these two emission components show very dissimilar temperature dependence in addition to their different peak positions and even different lineshape.[19] In the present work we will address the electroluminescence signal transition from the superlattice-like delocalized states to the Anderson-type localized states in the GaInP-based single solar cell.

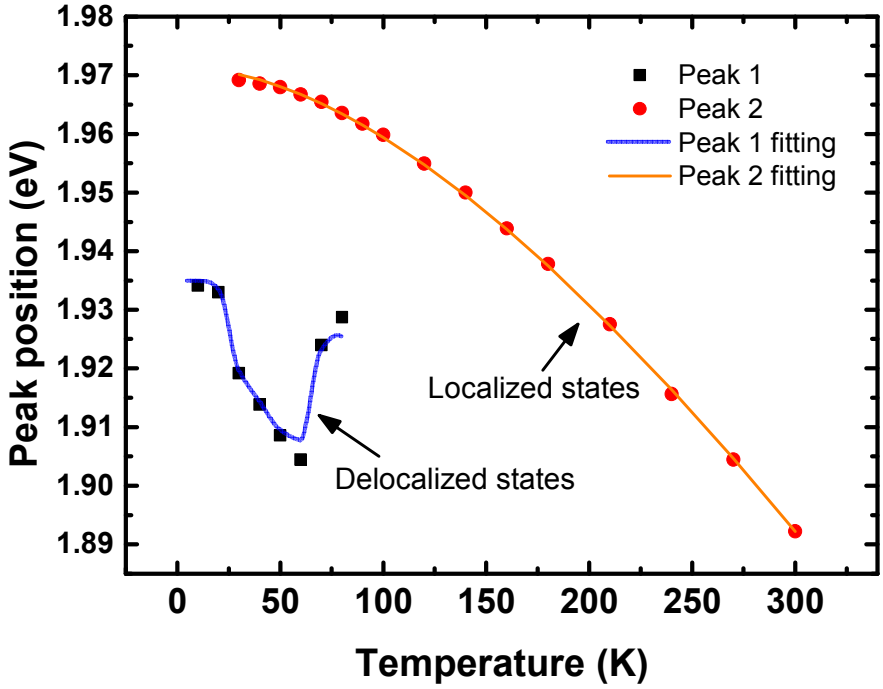

Fig. 3. Temperature dependence (symbols) of the peak positions of the two EL emissions depicted in Fig. 2. The solid lines are the theoretical fitting curves. For Peak 1, its peak position is fitted with the LSE model while that of Peak 2 is fitted with the Varshni's empirical formula.

In order to quantitatively interpret the commonly observed anomalous temperature dependence of luminescence of localized carriers, a generalized model, namely localized-state-ensemble (LSE) luminescence model was developed by us.[29, 30] According to this model, luminescence spectrum of localized carriers with a Gaussian-type density of states (DOS) reads[29]

$$I \propto \rho(E)\cdot f(E,T) = \rho_0 e^{-(E-E_0)^2/2\sigma^2}\cdot\frac{1}{e^{(E-E_a)/k_BT}+\tau_{tr}/\tau_r}, \quad (1)$$

where $\rho(E) = \rho_0 e^{-(E-E_0)^2/2\sigma^2}$ represents a Gaussian-type DOS due to the distribution of the localized states in energy space, E_0 is the central energetic location of Gaussian-type DOS, E_a is a characteristic energy level, k_BT is Boltzmann thermal energy, and $\tau_{tr}(\tau_r)$ represents the time constant of carrier escaping (radiative recombination) from the localized states. By seeking for the maximum value of the expression in the right hand side of Eq. (1) with respect to temperature, we obtain a modification term to the Varshni's empirical formula for luminescence peak position. Finally the luminescence peak position of localized carriers can be formulated as[18, 29]

$$E(T) = \left(E_0 - \frac{\alpha T^2}{\theta + T} \right) - x \cdot k_B T \,, \tag{2}$$

where θ is Debye temperature and α is the Varshni parameter, and x is a dimensionless parameter which can be yielded by numerically solving the following equation[18, 29]

$$xe^x = \left[\left(\frac{\sigma}{k_B T} \right)^2 - x \right] \left(\frac{\tau_r}{\tau_{tr}} \right) e^{(E_0 - E_a)/k_B T} \,. \tag{3}$$

V-shaped temperature dependence of peak position of Peak 1 was fitted with the LSE model briefly described above, and the fitting curve was depicted in Fig. 3. For the best fitting, various parameters with values of $E_0 = 1.935$ eV , $\alpha = 6.989 \times 10^{-2}$meV/K , $\theta = 450$ K , $E_a = 1.956$ eV , $\tau_{tr} / \tau_r = 3.684 \times 10^{-2}$ and $\sigma = 26.0$ meV were adopted. Temperature dependence of peak position of Peak 2 was found to follow the tendency described by the Varshni's formula. As depicted by solid line in Fig. 3, the best fitting was yielded with the Varshni's formula for $E_0 = 1.971$ eV and $\alpha = 0.659$ meV/K . This may be ascribed to the negligible thermal redistribution of carriers within this group of localized states with large density of states.

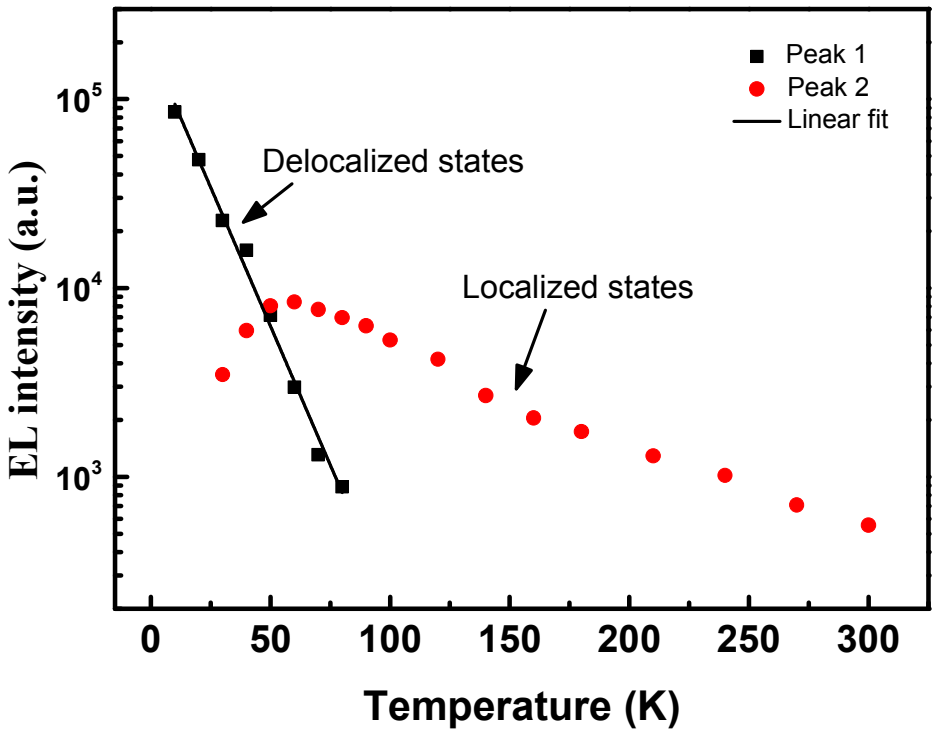

Fig. 4. Intensities (solid symbols, depicted in semi-logarithmic scale) of Peak 1 and Peak 2 versus temperature. The solid line is the least-square linear fitting to the logarithmic intensity of Peak 1.

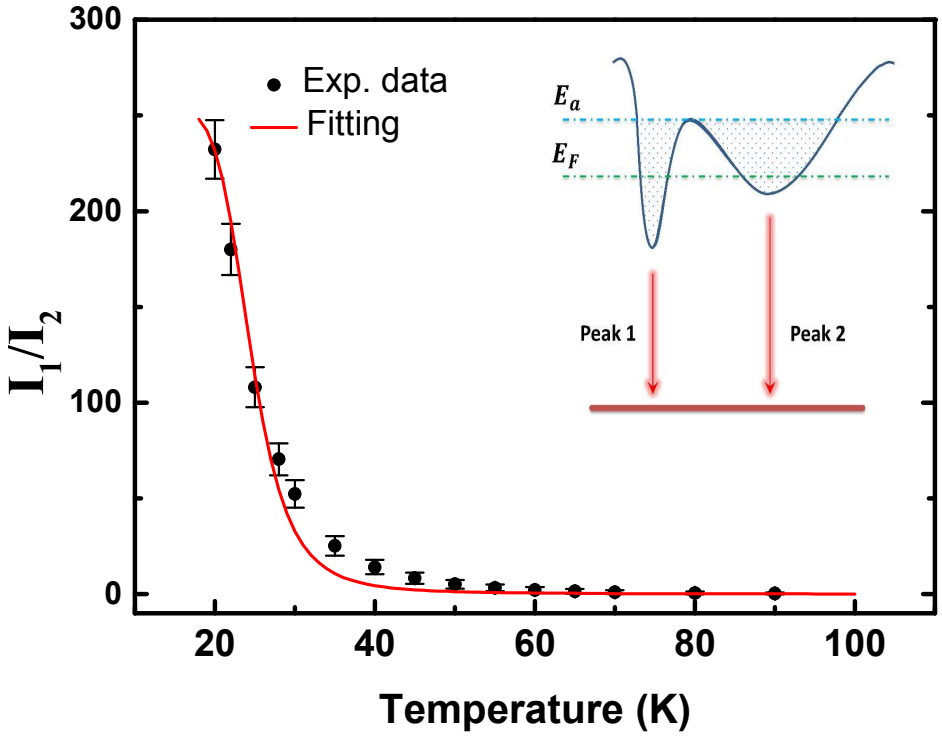

Fig. 5. Temperature evolution of ratio of integrated intensity of two peaks from EL spectra. The inset is schematic energy band diagram.

Obviously, carrier transfer from the delocalized states to the localized states is a temperature-dependent dynamic process. Such carrier transfer shall result in fast attenuation of Peak 1 intensity and increase of Peak 2 intensity at least within a certain temperature range. As seen in Fig. 4, indeed, the Peak 1 intensity (solid squares) exhibits a fast exponential decay while the Peak 2 intensity (solid circles) increases first, reaches its maximum at 60 K, and then experiences a slower exponential decay, as the temperature increases. Assuming that thermal transfer of carriers between the two groups of electronic states is a major physical mechanism, temperature dependence of the integrated intensity ratio of the two emission bands can be derived from the rate equations as[31]

$$\frac{I_1}{I_2} = \frac{R_1}{R_2} \frac{U_0}{\left(R_{n1} + R_1 T^{-2} + U_0 e^{-E_t/k_B T}\right)}, \quad (4)$$

where $I_1(I_2)$, $R_1(R_2)$, $R_{n1}(R_{n2})$ are the integrated intensity, radiative recombination rate and nonradiative recombination rate of Peak 1(Peak 2), respectively, U_0 is the trapping rate, and E_t is the transfer barrier between the two recombination channels. The best fitting result with Eq. (4) was obtained by taking $R_1=2.28\times10^8 s^{-1}$, $R_2=1.65\times10^8 s^{-1}$, $R_{n1}=1.79\times10^9 s^{-1}$, $U_0=5.98\times10^{13} s^{-1}$, and $E_t=22.0\ meV$, as depicted by the red solid line in Fig. 5. Very good agreement between theory and experiment is achieved, suggesting that carrier transfer between the two groups of electronic states is indeed a main physical mechanism in the studied GaInP alloy.

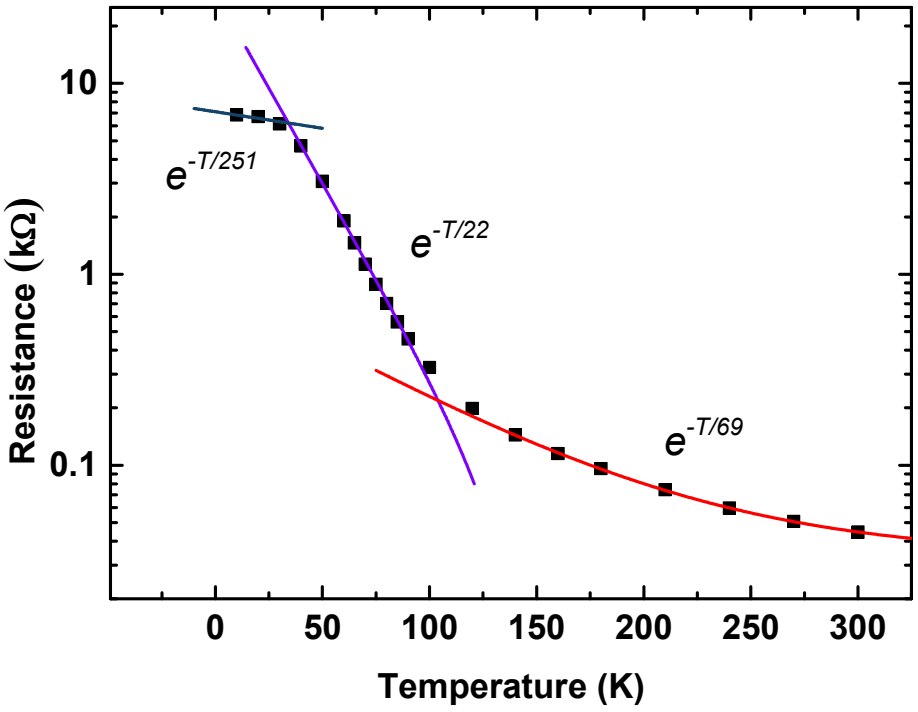

Fig. 6. Temperature evolution (solid squares, depicted in semi-logarithmic scale) of the electrical resistance of the sample. The solid lines are the exponential fitting results.

After having above-described model simulations to the experimental data, now we turn to give a more detailed discussion on the two kinds of electronic states well as carrier transfer between them. As argued in the introduction part, carrier localization shall be a common phenomenon in partially disordered isovalent ternary semiconductors including GaInP alloy studied in the present work. In addition to the compositional fluctuations in indium (gallium) content within the alloy layer,[32, 33] local atomic ordering domains with different ordering degrees may exist.[26, 34] Very recently, Li *et al*. suggested that two kinds of localized states induced by In-rich clusters

with varying indium contents and QW structures with different well widths, respectively, result in the two distinct emission peaks in a green InGaN/GaN MQW LED structure.[35] In fact, spontaneously partially ordered GaInP alloy could be phenomenologically described as a disordered GaInP matrix embedded with local atomic ordering domains.[19] The remarkable V-shaped evolution of peak position of Peak 1 upon temperature is usually regarded as a typical carrier localization effect.[18, 28, 29] It needs pointing out that the wave functions of electronic states are actually locally extended in the superlattice-like lattices of local ordered domains. In contrast, Peak 2 is associated with the localized states having higher eigenenergy, although they are quantum-mechanically localized in the disordered region. The situation looks strange, but it is reasonable and self-consistent. We thus have a physical picture giving a phenomenological but self-consistent description of the two groups of electronic states and corresponding emission channels in the GaInP alloy, as shown in the inset figure in Fig. 5.

As the carrier transfer and luminescence mechanism transition were observed in the GaInP alloy, a characteristic energy barrier or boundary shall exist between the groups of electronic states. In the LSE model, $E_a - E_0$ is argued to be a key parameter and act as an energy barrier or thermal activation energy.[29, 30] At 10 K, $E_a - E_0 = 21.3\,meV$ was obtained for the best fitting with LSE model. When we used Eq. (4) to do fitting, we obtained a transfer barrier of E_t=22.0 meV. The two values are nearly equal to each other. This fact makes us believe that the energy barrier between the delocalized states and localized states in the studied GaInP alloy is about 21 meV. To make further investigation on the influence of carrier localization and transfer, we measured the electrical resistance of the solar cell sample at different temperatures. The results (solid squares) are depicted in semi-logarithmic scale in Fig. 6. It has been shown that exponential decrease of the electrical resistance of a disordered electron system with respect to temperature is a typical effect of Anderson localization.[36] It is obvious that the electrical resistance evolution of the sample with temperature can be divided into 3 regions. This is consistent with the behavior of the luminescence transitions. Below 30 K, only Peak 1 is observable. Correspondingly, the electrical resistance exponentially decreases in a slow rate, which is mainly related to the occupying of local extended states. From 40 K to 90 K, significant transfer and thermal redistribution of carriers between the two kinds of electronic states take place, which results in rise of concentration of conductive carriers, and thus quick decrease of the resistance is observed. When the temperature gets higher than 100 K, Peak 1 almost completely quenches and the carriers mainly occupy the Anderson-type localized states. Consequently, the electrical resistance of the sample exponentially decreases in a slower pace again.

Conclusions

In conclusion, transition of radiative recombination mechanism of carriers from local extended states to Anderson localized states in partially ordered GaInP alloy was revealed by employing a GaInP/GaAs single-junction solar cell and variable-temperature EL spectroscopic measurement. The spontaneous local InP/GaP superlattice domains and random distribution of indium content

are suggested to be responsible for the local extended states and Anderson localized states, respectively. It is found that the transfer and thermal redistribution of carriers between the two groups of electronic states cause the transition of luminescence mechanism and account for the anomalous temperature dependent behaviors. A transfer barrier of ~21 meV was deduced from the fittings to the experimental data with two models. The electrical resistance of the sample also exhibits exponential decrease with increasing temperature. The study leads to a self-consistent and precise picture of carrier localization and luminescence mechanism in semiconductors with similar short-range ordering domains and long-range random matrix.

Acknowledgements

The study was financially supported by Natural Science Foundation of China (Grant No. 11374247).

References

1 P. W. Anderson, Phys. Rev., 1958, **109**, 1492.

2 E. Abrahams, P. W. Anderson, D. C. Licciardello and T. V. Ramakrishnan, Phys. Rev. Lett., 1979, **42**, 673.

3 P. A. Lee and D. S. Fisher, Phys. Rev. Lett., 1981, **47**, 882.

4 M. P. Van Albada and A. Lagendijk, Phys. Rev. Lett., 1985, **55**, 2692.

5 S. John, Phys. Rev. Lett., 1987, **58**, 2486.

6 T. Giamarchi and H. J. Schulz, Phys. Rev. B: Condens. Matter,1988, **37**, 325.

7 B. Kramer and A. MacKinnon, Reports Prog. Phys., 1993, **56**, 1469.

8 D. S. Wiersma, P. Bartolini, A. Lagendijk and R. Righini, Nature, 1997, **390**, 671.

9 F. Scheffold, R. Lenke, R. Tweer and G. Maret, Nature, 1999, **398**, 206.

10 T. Schwartz, G. Bartal, S. Fishman and M. Segev, Nature, 2007, **446**, 52.

11 J. Billy, V. Josse, Z. Zuo, A. Bernard, B. Hambrecht, P. Lugan, D. Clément, L. Sanchez Palencia, P. Bouyer and A. Aspect, Nature, 2008, **453**, 891.

12 G. Roati, C. D'Errico, L. Fallani, M. Fattori, C. Fort, M. Zaccanti, G. Modugno, M. Modugno and M. Inguscio, Nature, 2008, **453**, 895.

13 A. Lagendijk, B. van Tiggelen and D. S. Wiersma, Phys. Today, 2009, **62**, 24.

14 S. Karbasi, R. J. Frazier, K. W. Koch, T. Hawkins, J. Ballato and A. Mafi, Nat. Commun., 2014, **5**, 3362.

15 S. Karbasi, C. R. Mirr, P. G. Yarandi, R. J. Frazier, K. W. Koch and A. Mafi, Opt. Lett., 2012, **37**, 2304.

16 N. F. Mott and E. A. Davis, *Electronic Processes in Non-Crystalline Materials*, Oxford University Press, 2012.

17 S. H. Wei and A. Zunger, Phys. Rev. B: Condens. Matter, 1989, **39**, 3279.

18 Q. Li, S. J. Xu, W. C. Cheng, M. H. Xie, S. Y. Tong, C. M. Che and H. Yang, Appl. Phys. Lett., 2001, **79**, 1810.

19 J. Q. Ning, S. J. Xu, Z. Deng and Z. C. Su, J. Mater. Chem. C, 2014, **2**, 6119.

20 S. H. Wei and A. Zunger, Phys. Rev. B: Condens. Matter, 1994, **49**, 14337.

21 S. H. Wei and A. Zunger, Appl. Phys. Lett., 1994, **64**, 1676.

22 Y. Zhang, A. Mascarenhas and L.-W. Wang, Phys. Rev. B: Condens. Matter, 2001, **63**, 201312(R).

23 J. Shao, R. Winterhoff, A. Dörnen, E. Baars and J. H. Chu, Phys. Rev. B: Condens. Matter, 2003, **68**, 165327.

24 F. Dimroth, M. Grave, P. Beutel, U. Fiedeler, C. Karcher, T. N. D. Tibbits, E. Oliva, G. Siefer, M. Schachtner, A. Wekkeli, A. W. Bett, R. Krause, M. Piccin, N. Blanc, C. Drazek, E. Guiot, B. Ghyselen, T. Salvetat, A. Tauzin, T. Signamarcheix, A. Dobrich, T. Hannappel and K. Schwarzburg, Prog. Photovoltaics Res. Appl., 2014, **22**, 277.

25 V. K. Khanna, *Fundamentals of Solid-State Lighting: LEDs, OLEDs, and Their Applications in Illumination and Displays*, CRC Press, 2014.

26 S. Smith, H. M. Cheong, B. D. Fluegel, J. F. Geisz, J. M. Olson, L. L. Kazmerski and A. Mascarenhas, Appl. Phys. Lett., 1999, **74**, 706.

27 Z. Deng, J. Q. Ning, Z. C. Su, S. J. Xu, Z. Xing, R. X. Wang, S. L. Lu, J. R. Dong, B. S. Zhang and H. Yang, ACS Appl. Mater. Interfaces, 2015, **7**, 690.

28 Z. Deng, R. X. Wang, J. Q. Ning, C. C. Zheng, W. Bao, S. J. Xu, X. D. Zhang, S. L. Lu, J. R. Dong, B. S. Zhang and H. Yang, Sol. Energy Mater. Sol. Cells, 2013, **111**, 102.

29 Q. Li, S. J. Xu, M. H. Xie, and S. Y. Tong, Europhys. Lett., 2004, **71**, 994.

30 Q. Li, S. J. Xu, M. H. Xie, and S. Y. Tong, J. Phys.: Condens. Matter, 2005, **17**, 4853.

31 S. J. Chua, S. J. Xu, X. H. Zhang and X. Zhang, Microelectron. Eng., 1998, **43-44**, 287.

32 M. Sugisaki, H. W. Ren, K. Nishi, S. Sugou and Y. Masumoto, Phys. Rev. B: Condens. Matter, 2000, **61**, 16040.

33 S. De, A. Layek, A. Raja, A. Kadir, M. R. Gokhale, A. Bhattacharya, S. Dhar and A. Chowdhury, Adv. Funct. Mater., 2011, **21**, 3828.

34 H. M. Cheong, A. Mascarenhas, J. F. Geisz, J. M. Olson, M. W. Keller and J. R. Wendt, Phys. Rev. B:Condens. Matter,1998, **57**, R9400.

35 Z. Li, J. Kang, B. W. Wang, H. Li, Y. H. Weng, Y. C. Lee, Z. Liu, X. Yi, Z. C. Feng and G. Wang, J. Appl. Phys., 2014, **115**, 083112.

36 C. M. Soukoulis and E. N. Economou, Waves in Random Media, 1999, **9**, 255.